Machine learning algorithm, simulation for 3D tracking of a needle with integrated ultrasound sensor within a 2D ultrasound imaging field

Supervisors:

Wenfeng Xia
Faculty of Life Sciences and Medicine
King's College London

Christian Baker
Faculty of Life Sciences and Medicine
King's College London

Participants:

Haowen Ma
Faculty of Life Sciences and Medicine
King's College London

Jiaqi Li
Faculty of Life Sciences and Medicine
King's College London

Ziming Liu
Faculty of Life Sciences and Medicine
King's College London

Timothee Caussin
Faculty of Life Sciences and Medicine
King's College London

Wenzhuo Sun
Faculty of Life Sciences and Medicine
King's College London

Abstract*—Needle-based intervention is a commonly used clinical technique for interbody testing or tissue sampling, where precise positioning of the needle is important to protect the patient from accidental injury. The aim of this paper is to address the problems associated with distortion of needle position in chorionic villus sampling (CVS) and amniocentesis (AC) testing. Based on the fibre-optic hydrophone (FoH) and US image needle tip guiding system designed by Baker. C, we try to predict the next moment of needle movement by starting with two aspects of the system: FoH position prediction and US image prediction, different neural network systems: Convolutional neural networks (CNN) and U-net will be used to train and fed data will be obtained using MATLAB's k-wave toolbox to simulate the FoH work in underwater condition. The results show that for ultrasound based predictions, an accuracy of 77.14% within a threshold of 10mm is obtained and the FoH based predictions achieves average accuracy of 13.9mm in CNN and 5.16mm in U-net. Finally, the upgrade of the system to tracking in 3D case was discussed and possible suggestions for future work were made.

I. Introduction

A. Background information

Ultrasound (US) is a medical imaging technology that uses high-frequency sound waves to scan the human body and visualize the internal structures [1]. This non-invasive and safe diagnostic tool is used widely in various medical fields to diagnose and monitor conditions, guide procedures, and has becoming increasingly standard practice for needle-based interventions, such as regional anesthesia and endoscopy [2],[3]. However, due to the unique circumstances of these procedures, it is essential that human safety is guarded when operating. For a long period of time, these procedures have been performed by experienced surgeons under the guidance of ultrasound and various medical technologies. Even through, fully ensuring patient's safety during operation are still challenging. Plenty of solutions have already been proposed. However, few adequate solutions emerged and there is still potential for improvement in relevant research. This paper, therefore, will attempt to improve on existing research. Baker. C and Xia have proposed a real-time ultrasound needle tracking system based on integrating a fibre-optic hydrophone (FoH) and US image guiding [4],[5]. It can be used to detect the true position of needle tip and expose the interior image to users. fibre-optic hydrophone is a component which can convert acoustic pressure value into time-varying voltage signal proportionally. From [5],[6], FoH is embedded into needle tip and corresponding algorithm has been designed to detect the needle tip which been visualized on the US image screen.

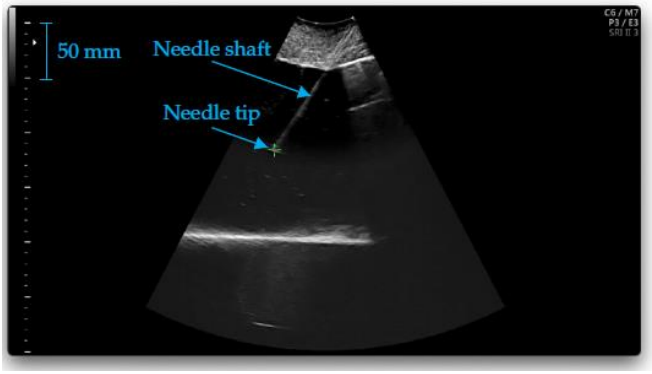

Fig. 1. US image on screen [4].

The figure above illustrates the US image appear on screen with the result of FoH detection. The green cross will always be following the needle tip and gives its position.

However, this is only available in 2D case, the real working environment is supposed to be three-dimensional, current research is not perfect for deployment. This research will mainly focus on starting with a 2D working field, aiming at attempting predict the position of the needle in the 3D case by way of data driven and algorithms development.

MATLAB simulation will be used to acquired data of FoH and two machine learning models will be explored and presented. The results will be analysed and compared from different perspectives.

B. Clinic problem and Motivation

For surgical procedures where the needle needs to be placed precisely in a specific area of the body, the exact needle tip position is critical. Needle tissue acquisition is an important procedure to detect the condition of human such as fetal medicine and tumour biopsy [7]. For the former, two of the most typical procedures are chorionic villus sampling (CVS) and amniocentesis (AC) test. The position of the needle tip during this procedure is much more critical. Pregnant mothers need to be tested for either CVS or AC between 8-12 weeks after pregnancy in order to find out if the baby has any physical defects or congenital diseases which is morally and healthily necessary [8]. By European Surveillance of Congenital Anomalies (EUROCAT) [9],[10]: 88% of babies with congenital diseases were detected. As evidenced, pre-conception testing is an extremely important part of the pregnancy process. However, during operation, nerve damage, organ injury or pregnancy loss may happen. 6% of procedures fail and need to be repeated and fetal loss rates of 1.4% for AC and 1.9% for CVS [4],[11]. For patients, some pregnant are therefore, negative towards these procedures. Also, any complications that arise during the procedure could lead to additional costs for both patients and healthcare providers. These challenges are usually resulting not only by operator experience, also equipment limitations and patient anxiety. To address it within medical equipment field, with the motivation of increasing the confidence of patients towards this operation and potentially reduce healthcare costs while improving patient outcomes. This paper will show the work by utilizing the latest technological advancements in medical equipment, to improve patient confidence and ultimately contribute to better overall healthcare outcomes for pregnant women.

C. Literature Review

The position of the probe affects the needle's visibility in ultrasonic images. A significant specular reflection happens when the imaging plane is parallel to the needle's direction [12]. Additionally, the ultrasound picture of the needle has linear artifacts [13].

A number of strategies have been put out over the past 30 years to try and nail down the location of the needle under ultrasonography. Through the use of spatial compounding, some studies have addressed reflections and artifacts. One such technique is the beam steering technique for standard needles, which adaptively steers the US beam at an angle perpendicular to the needle [14].

Additionally, several researchers have looked at the use of "Echogenic Needles," which are specially designed needles with echogenic coatings or indentations, to increase the needles' visibility in ultrasound pictures. [15,16,17]. Studies have also looked at ways to improve the beam steering technique used to create ultrasound images, maximizing the strength of the needle's reflection and enhancing the needle's visibility in the image [18]. Other studies have concentrated on improving machine learning algorithms for needle tip detection [19,20,21,22]. Although the accuracy rates in each of these trials were good, additional efforts are still required to reliably and precisely find the needle tip.

Improvements to the needle, such as the insertion of sensors or cameras, have been extensively used in active needle tracking studies in recent years [23,24]. Mohammad N. proposed a single camera closed-form needle tracking method by needle with identified markings and camera parameters [24]. However, this method relies on identified markings and has a total error of 3.0 ± 2.6 mm.

Electromagnetic tracking systems are among the more recent emerging needle tip tracking approaches [25,26]. A few sources, including noisy electronic equipment and large metallic or ferromagnetic structures, can produce EM field distortion, which is especially sensitive to EMTS [27]. The proportional significance of the generated deformation has been demonstrated to vary on the size, composition, proximity, and shape of the items under consideration [28,29,30].

Additionally, there are numerous attempts to increase the visibility of sonographic needles, such as the creation of dimples or echogenic coatings on specific needles. The "Cornerstone" reflectors that have been machined into the needle surface, which typically cover the distal end of the cannula, increase the reflected echo from the needle end and increase visibility [31]. Such echogenic needles have been shown to improve needle visibility [15], but because they are frequently more expensive, there is a lower likelihood that they will be extensively used. As of right now, the majority of needles intended for clinical usage are still constructed of gleaming stainless steel and include steel or plastic styluses (solid detachable cores inside the needles).

A fiber optic hydrophone (FoH)-based ultrasonic tracking technique was recently proposed by Baker, C., and Xia [4]. This method transforms the temporal ultrasonic signal that the needle tip receives. The device converts the temporal ultrasound signal the needle tip receives into a spatial location using a fiber-optic hydrophone, allowing for the real-time production of the needle tip's 3D position in a 2D ultrasound image [4].

II. Methodology

In order to be able to precisely predict the needle's position in the ultrasound plane, we aim at developing neural networks using FoH and ultrasound data acquired by the system in real time. The end goal would be to be able to develop a single algorithm that can combine ultrasound and FoH measurements into a single prediction. However, we were not able to implement this combined neural network and focused on independent networks based respectively on ultrasound and FoH data to predict needle positions. We will later discuss how these networks could be combined.

A. Training data

The training data used to train the neural networks has been acquired according to the experiment described in [4]. This experiment allowed to acquire ultrasound and FoH frames for 462 different needle positions. The following figure displays all the needle positions that have been tested.

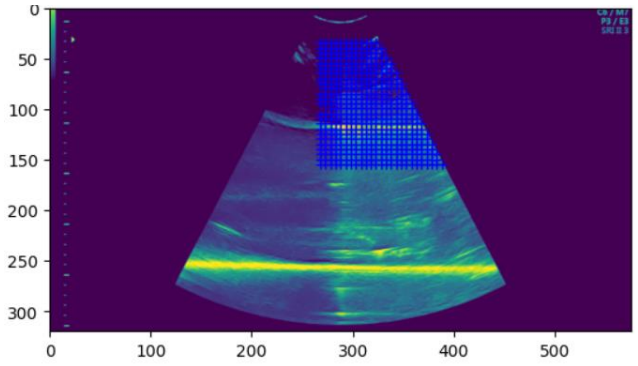

Fig. 2. Needle Position in the Ultrasound Frame.

Each ultrasound frame consists of an array of 800x1440 with an isotropic pixel size of 0.4mm. Each FOH frame consists of an array of 3896x124. The x axis represents the 124 different elements in the ultrasound frame and the y axis represents the time that each waveform takes between its emission and reception by the ultrasound probe. The system of coordinates of FoH frames can be interpreted as polar coordinates where the probe element represents the angle, and the time represents the distance from the center of curvature. The needle's position in the FoH frame can therefore be computed from its position in the ultrasound frame using cartesian to polar transforms.

As neural networks are often limited by the size of the dataset, we have decided to also implement a simulation method that would allow to simulate FoH data for each needle position.

B. MATLAB Simulation

- Purpose:

The main aim of the project is to produce an AI algorithm for 2D needle tracking. With the help of the supervisor, much of the data measured using the instrument has been obtained and can be used directly to train the AI model. However, we were not satisfied with just using the experimental data provided. So, we used MATLAB and an open-source toolbox, K-Wave [32], to perform and record simulation data from the hydrophone's simulations for AI training purposes.

- Simulation Setup:

In order to simulate a realistic ultrasound test as closely as possible, the simulated area was set up in water, so that the speed of sound waves in the water was 1540m/s.

The 192 transducers are placed in a semi-circular layout in front of the source. Only some of the transducers are activated at a time to focus the ultrasound in a certain direction at a specific location. In our simulations, the ultrasound waves are scanned from the right side to the left side, with a total of 124 scan lines generated by the 192 transducers.

In addition to setting the position of the transducers, we also need to set the position of the hydrophone to receive the water pressure generated by the ultrasound. We can place the hydrophone array at random within the simulation area to obtain water pressure data at different locations. As shown in the figure below, the semi-circular area on the way is the transducer array with the ultrasonic source, and the triangle in the simulation area is the hydrophone array. The red areas in the diagram are the activated transducers and the black areas are the inactive transducers. The red dashed line is the theoretical beam axis and the green cross is the current theoretical focal position of the active A-line. The MATLAB code for this simulation is from Christian Baker [33], a researcher at KCL.

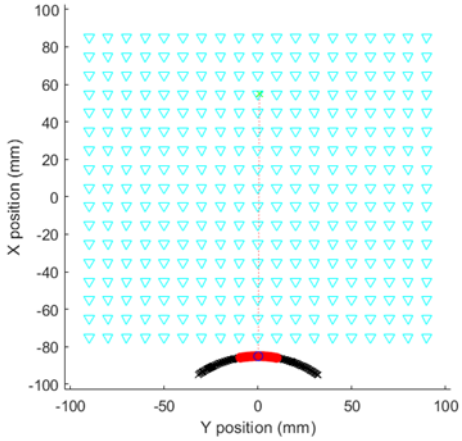

Fig. 3. MATLAB Simulation Setup

- Simulation Result:

After the setup is complete, we can start the simulation. The simulation takes a long time and once it is complete, we can obtain the water pressure data generated by the ultrasound for each hydrophone we have placed during the entire simulation. The key to the simulation is the choice of simulation mode. In order to provide data for the AI training, we chose to use waveform mode, which allows us to record the pressure data for each hydrophone individually. The result obtained is shown in the figure below.

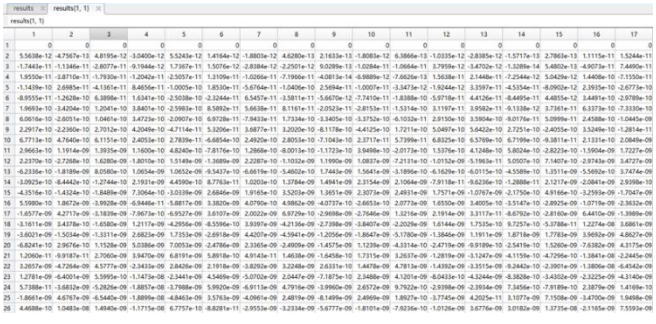

Fig. 4. Pressure Value Recorded

Each column in the graph shows all the pressure data collected by one hydrophone and each row shows the pressure data for each hydrophone at the current time. The size of the data set depends on the number of hydrophones set up and the length of the simulation. This data can be used for training of the AI model, if it is correctly transformed into the appropriate format to be read by the training script. In our project, all simulation data was converted into h5 file format.

In addition to this, the simulation code provides the RMS (Root of mean square) mode, where the data obtained will be the root of mean square pressure value for each

point in the simulation area throughout the simulation instead of pressure value record by each hydrophone. From this we can obtain a dynamic diagram of the propagation of the ultrasound through the water, which gives a better picture of how it works (shown in figure below).

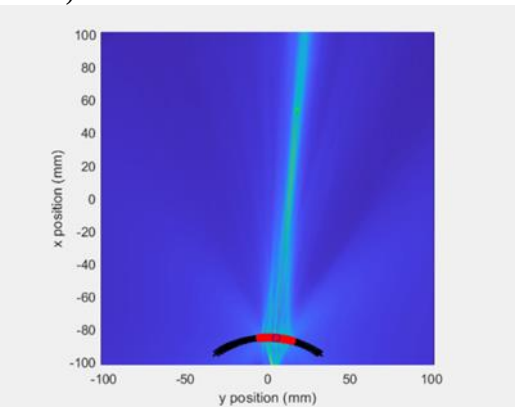

Fig. 5.Graph Generated by RMS Value

- Shortcomings:

This simulation was carried out using off-the-shelf code and simulation data was obtained. However, there were some shortcomings. The most obvious part of the simulation is the consistency of the simulation area, which is all water, which is not consistent with the structure of the human body, as the human body is not only made up of fluid, but various tissues such as muscle and fat have different densities and sound waves travel at different speeds through them. With the rest of the data being experimental, this could affect the training results. There is of course a solution to this problem. We can add an appropriate amount of noise to the simulated data obtained, which will improve the training of the AI model while ensuring that most of the data is reliable. There is also the issue of how to convert the obtained data into h5 format correctly, as all experimental data has a fixed format and the AI training scripts are based on the experimental data, so if the simulated data cannot be stored correctly it cannot be used for AI training.

C. *Network architecture*

- Ultrasound based predictions:

An algorithm for needle position prediction based on a 2-dimensional ultrasound image dataset was developed using PyTorch. The algorithm uses convolutional neural networks (CNNs) model as the basis for implementing supervised learning tasks[34]. A model structure named 'NeedlePositionPredictor' consists of three sets of layers: convolutional layer, ReLU activation, and max pooling, each set increasing the number of filters from 16 to 32 to 64. After these, a flattening operation is performed to prepare the data for fully connected layers. Next, two fully connected layers with ReLU activations are applied, with 512 and 128 neurons respectively. Finally, an output layer with 2 neurons is used to predict the two positional coordinates of the needle, shown in Fig.6.

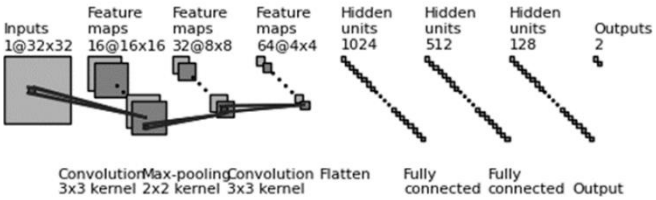

Fig. 6. "NeedlePositionPredictor" Model architecture

The overall pipeline implementation includes loading image and position data from a file. Splitting the data into a training set, a validation set and a test set (70%-15%-15%). Obtaining random image flip states for both the horizontal and vertical axes from a custom ultrasound dataset and applying the same flip transformation to position data[34][35]. And using random horizontal and vertical flip transforms, random rotation and random affine transforms to the training set to achieve data enhancement. A convolutional neural network model called NeedlePositionPredictor (a CNN-based model architecture[34][36]) is defined. The model is trained by using a Mean Absolute Error loss function and an Adam optimiser with a learning rate of 1e-4 and a weight decay of 1e-3 in 300 epochs. The Mean Square Error (MSE[36]), Mean Absolute Error (MAE[37]) and Average Euclidean distance metrics were used to evaluate the model on the test set. Creation of a scatter plot of the predicted position compared to the true position and a dynamic visualisation of the true position of the needle on the track compared to the predicted position, shown in Fig.7

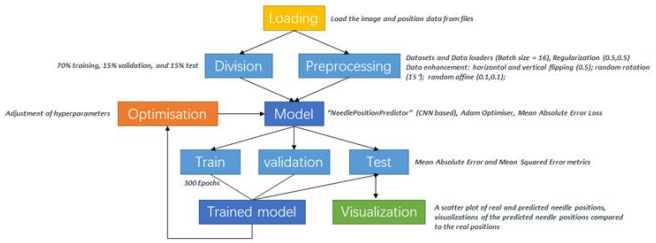

Fig. 7. Pipeline implementation structure

For the optimisation part, the learning rate was adjusted to an adaptive learning rate and the random affine parameter in the data enhancement was adjusted to 0 degrees, the value of translation was set to (0.1, 0.1), the value of random rotation was set to 15 degrees and the flipped data were all set to a 50% probability.

- FOH based predictions:

Two different networks were implemented in order to predict the needle's position from FOH data.

The first network is a simple convolution network taking a 2D FoH frame as input and giving the predicted needle coordinates as output. This network firstly features 4 layers which are all made of a convolution function, an activation function (Relu) and a max pooling function. The convolution kernels are of size (7,5,5,5) with channels of size (20,50,150,2). This structure allows to extract key information from the image while reducing its dimension.

After these 4 convolution layers, the data is flatted and fed into a fully connected network. This network is made of 3

layers with respectively 1434,512 and 2 neurones. The final 2 neurones represent the x and y coordinates of the needle. This network is displayed on Fig. 8.

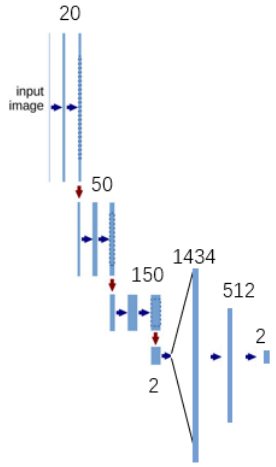

Fig. 8. Architecture of the CNN Model.

The main advantage of a CNN network is its simplicity and quick training time. The model was trained using a MSE loss and Adam optimiser with a learning rate of 10^{-3}. The second network that was implemented is a U-net. The U-net that was implemented featured 5 layers with channels of size (32,32,64,128,256) and can be seen on Fig. 9. Its goal was to bypass the need to explicitly compute coordinates by creating probability maps of the position of the needle instead. The input is therefore the same as for the CNN but here the output is now a 2D probability map following a gaussian distribution centered on the real position of the needle. This change in data type requires a different loss function. A Binary Cross Entropy loss was used.

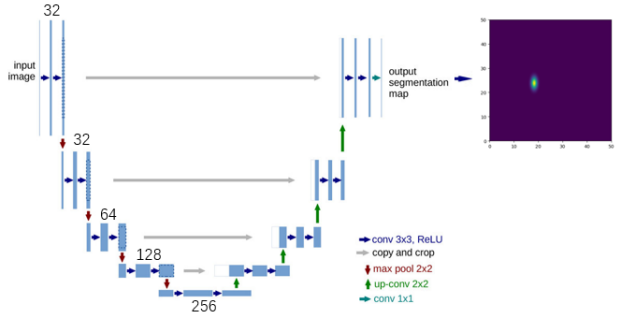

Fig. 9. Architecture of the U-net Model.

This new architecture introduces more complexity to the network but also introduces new hyper-parameters. Indeed, we now need to define σx and σy, the standard deviation of the gaussian distribution in the x and y direction. We also have to introduce a new algorithm to extract the needle position from the probability maps. The simplest approach to do so is to compute the coordinates of the maximum intensity point. In the case of a perfect gaussian output from the U-net this method would work. However, it would not be robust to error and could be improved.

III. Results

A. *Ultrasound based predictions*

After 300 epochs of training, the final training loss was 22.314 and the validation loss was 20.46, indicating that there was some overfitting of the model in training, possibly because there was too little data causing the model to learn too well and generalise poorly, shown in Fig.10. It is also possible that the model architecture is not complex enough and needs to be optimised. This could be considered by continuing to tune the hyperparameters of the model to find the best configuration or applying dropout to the model architecture to prevent overfitting to help the model generalise better. Alternatively, there may be some noise in the data itself that is causing errors in quality. For the data enhancement part, several data enhancement methods are used and other data enhancement methods suitable for 2D data, such as contrast, distortion or Gaussian noise and denoising.

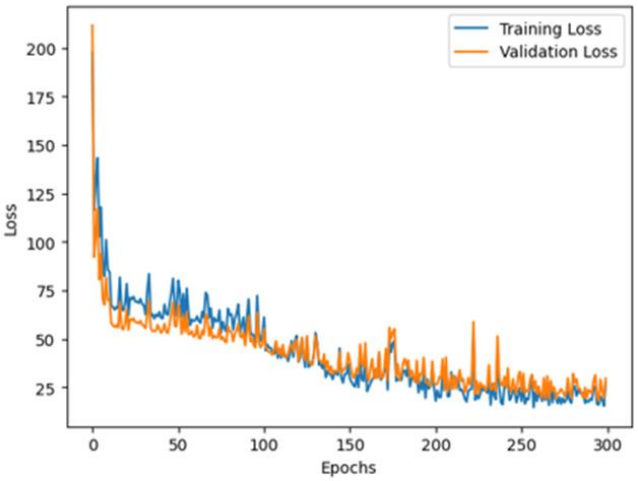

Fig. 10. Training & validation loss map.

In testing, the needle position has been converted to a pixel position in ultrasound. For the results of the scatter plots of the true and predicted needle positions, we can see by the performance in the test set that the model produces predictions of the needle positions (x and y) in 300 epochs as expected. The average Euclidean distance is 9.92mm, which indicates that the predictions are generally in line with the requirements, but there is still some error between the predictions and the reality, shown in Fig.11.

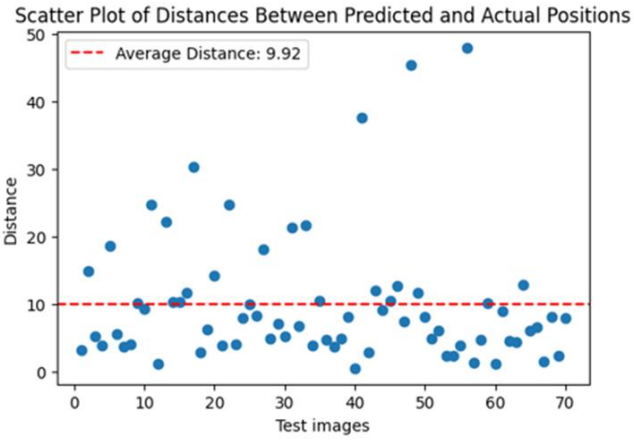

Fig. 11. Scatter Plot of Distances Between Predicted and Actual Positions.

Based on the validation losses and evaluation metrics, the model appears to perform reasonably well on the test data. The average absolute error was 6.37 mm, and the average squared error was 9.7146 mm. Also, based on the result of the track map, we can find that most of the predictions are close to the true values, but there are some locations with large errors between the true and the predictions, shown in Fig.12. In summary, this shows that the model makes predictions that are relatively close to the true values. However, optimisation is still needed to achieve better optimisation results.

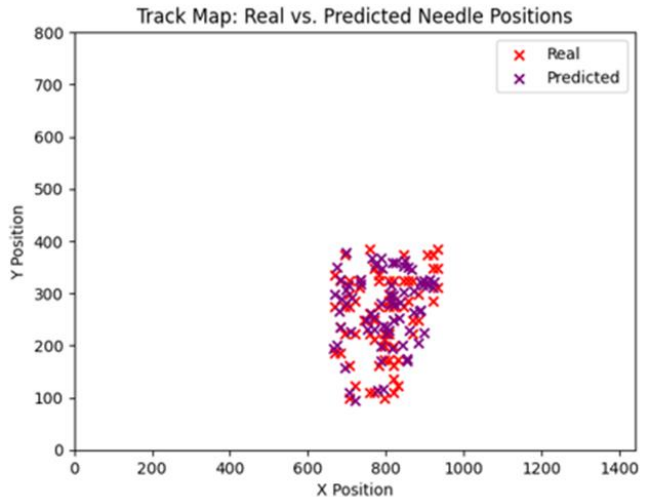

Fig. 12. Track Map: Real vs. Predicted Needle Positions.

Based on the results of a dynamic visualisation comparing the predicted position with the true position, shown in Fig.13, there are still some forecast deviations present. For this case a threshold value of 10 mm was set below which predictions were considered to be largely successful. Comparison with the true position of the needle on a test set of 70 images showed an accuracy of 77.14%, essentially achieving the aim of using ultrasound images for needle prediction.

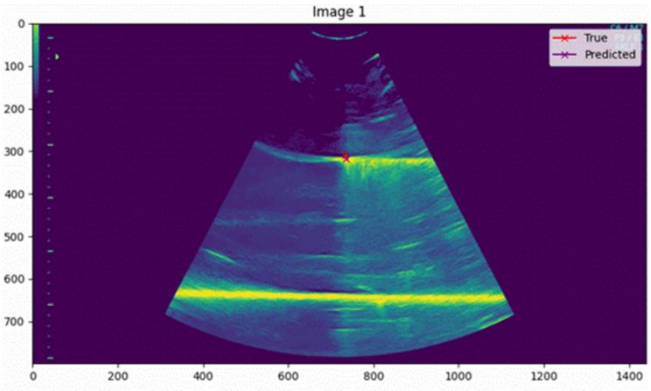

Fig. 13. A sample of true and predicted locations.

B. *FoH based predictions*

Both networks were trained until convergence of their loss function. After training on a testing and validation set, the networks were evaluated using an independent testing dataset.

In order to evaluate their results and be able to compare them to each over, the predictions from the U-net that were initially in the FoH domain (polar coordinates) were transformed back to cartesian coordinates to plot the graphs on Fig.14. The CNN achieved an average accuracy of 13.9mm and the U-net achieved an average accuracy of 5.16mm.

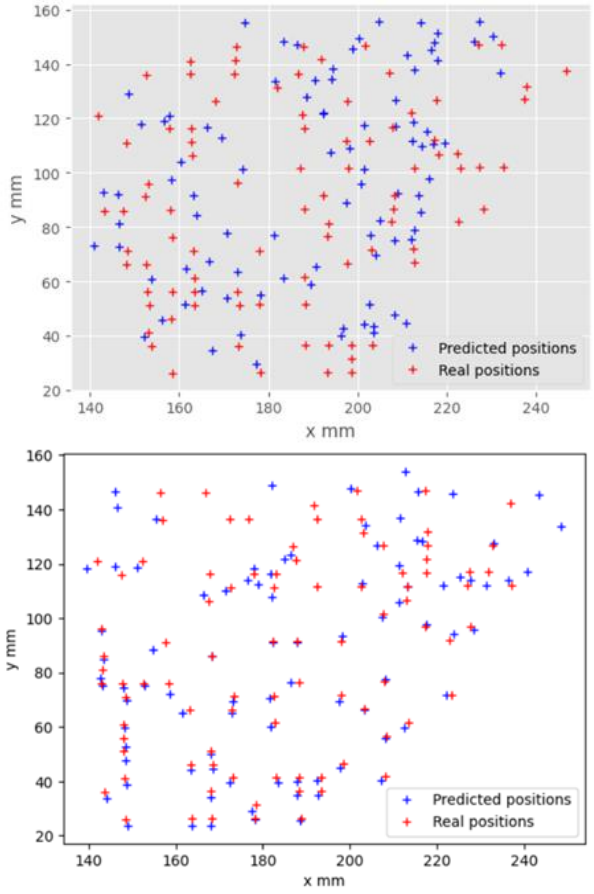

Fig. 14. Results for the U-net and CNN Models.

We can see that the CNN struggles to precisely predict the position of the needle. This can be explained by the fact that the CNN does not have any knowledge of the coordinates were are trying to predict. The network is only given the intensity of the FoH frame and there is no direct relationship between those intensities and the coordinates of the needle. This is the reason why the U-net performs better as it does not need to know the coordinates of the predicted point but only its relative position in the frame. In the case of the U-net, the computation of the coordinates is done manually when extracting the maximum intensity point coordinates from the probability map.

Looking at the results of the U-net, we can also see that there is a clear loss in precision as the depth of the needle increases. This can be due to the lower quality of the ultrasound data collected but is most likely due to the fact that the U-net works in polar coordinates with very low resolution on the angular axis (only 124 pixels for 55°). Therefore, as the depth increases, the euclidian distance between two points with different angles increases significativelly.

IV. Discussion

A. *Ultrasound based predictions*

This study developed a needle position prediction algorithm using a convolutional neural network (CNN) model based on two-dimensional ultrasound images. The model was trained on a custom ultrasound dataset and evaluated using various metrics, including Mean Square Error (MSE), Mean Absolute Error (MAE), and Average

Euclidean distance. After 300 epochs of training, the model performed reasonably well on the test data, with an average Euclidean distance of 9.92mm between the true and predicted needle positions and an accuracy of 77.14% for needle position predictions within a threshold of 10mm. The findings of this study are promising and suggest that CNN-based models can potentially be effective tools for needle position prediction in ultrasound-guided interventions and has potential for use in clinical practice. For the future work, increasing the size and diversity of the training data[38] could help to improve the model's ability to generalize and reduce overfitting. While CNNs are widely used for image processing tasks, other models such as recurrent neural networks (RNNs)[39] or "facial" concentric needle (FCNs)[40] could potentially be used. In cases where the performance of CNN-only models is not as good, integration techniques of multiple models can be considered[41]. These improvements will ultimately lead to the development of a system that can assist clinicians in the accurate and safe placement of needles during ultrasound-guided interventions, thereby improving patient outcomes.

B. FoH based predictions

The results of the U-net model show that reasonable accuracy can be achieved using AI to predict the position of a needle from FoH data. As a reference, using the same system with an analytical method, the average accuracy of the system was of 0.7mm.

The U-net model and algorithms used along with it could still be improved to achieve an average precision below 1mm. Firstly, the hyperparameters of the model could be optimised. Due to hardware limitations, a more complex structure of the U-net could not be tested in this project and increasing the number batch size of the number of channels could increase the final precision. Also, the standard deviation along x and y directions of the gaussian probability maps computed to train the model could be optimised. A smaller standard deviation for example would theoretically improve the model's precision but make the training more complex.

Concerning the low angular resolution of the system, the best improvement would be to train the U-net directly in the cartesian coordinate frame. This would avoid any transformations and approximations when computing needle positions in polar coordinates. This would however require modifying the architecture of the network to account for inputs and outputs of different dimensions.

As for all neural network's studies, this study would also benefit from a bigger dataset. This could be achieved by flipping all data points horizontally to simulate needle positions covering a larger area of the ultrasound frame. Using The Matlab script introduced earlier could also allow to increase the dataset. The model could for example be trained in two steps: firstly, learning on simulated data and then fine tuning the results on experimental data.

Finally, as we have mentioned earlier, the point detection algorithm to compute positions from probability map is very simple and is not very robust to errors from the U-net. A simple improvement could be to compute the centre of mass of the probability distribution instead of the position of the point with maximum intensity.

C. Combining both methods

In a real system, the real position of the needle would be unknown and there would be no way of choosing which method to use between FoH and US based needle position prediction. The best way around this problem is to design an architecture that would use both ultrasound and FoH data to compute a single position prediction.

There are two ways to do so using the work that has been presented so far. Firslty, one could aim at simply using a CNN with two channels as input (one for FoH and one for US data) to predict the needle's position. This would require an additional step, to convert FoH data to US data for example, to make sure that the size of the images and the information they carry is of similar nature. This conversion could be performed with a GAN architecture where a generative network would learn how to create FoH data from US.

The second way to use both data types would be to create two separate U-net models creating two probability maps. These probability maps would have to be converted to the same space and then summed using a weighted majority voting method for example. The weights could either be computed for each pixel or be computed for the entire map by comparing the output map to a perfect gaussian distribution.

V. CONCLUSION

We have improved the US image needle tip tracking system based on the fibre optic hydrophone (FoH) designed by Baker.C et al. by training a U-net with a time-varying voltage signal and an ultrasound image as input to achieve an average accuracy of 5.16 mm for the prediction of needle tip position. Feedback data was obtained using MATLAB's k-wave toolbox to simulate the operation of the FoH underwater. The system has been designed as an adjunct to clinical ultrasound surgery, with the hope of improving the success and efficiency of clinical procedures using ultrasound as an imaging modality. As the current experiments are underwater, future research will involve experiments with animals or simulated humans in order to translate the system into clinical use. Further machine learning models will also be trained and compared to the U-net.

In order to improve the experience for the surgeon using this system and lower the risks of complications, the system would need to be able to perform tracking outside of the ultrasound plane. Due to the loss of signal outside of the imaging plane, our models' performances would likely fall off the farther we are from the plane.

Looking at the literature on 3D tracking using freehand ultrasound, 3 different kinds of methods have been developed.

Firstly, using a 3D ultrasound probe, the ultrasound signal can be measured into FoH data similarly to what is done with our system. Even if this allows for 3D tracking, 3D probes come at a much greater cost and have a limited framerate due to the higher number of waveforms. Over systems using two and a half dimensions have also been developed [42] where a few elements of the probe emit out of the plane to allow for the needle's sensor to measure its position along the axis perpendicular to the plane.

Secondly, methods have been developed using a mechanical structure to force the needle to remain in the ultrasound plane throughout the operation [43]. This allows to use widely used ultrasound probes but require a custom robotic system that is often very expensive.

Finally, using machine learning, it is possible to compute the translation and rotation matrix that separate two successive

frames [44,45]. Such methods are usually based on speckle decorrelation [46]. These methods would allow to track the position of needle as long as it has been calibrated in the imaging plane [43]. The main disadvantage however is that they require to train a neural network on custom data acquired on a specific organ.

ACKNOWLEDGMENT

This research was supported by Prof. Wenfeng Xia and Mr. Christian Baker

REFERENCES

[1] Scoutt, Leslie M., et al. Ultrasound. Oxford University Press, 2017.

[2] Bowness J, Taylor A. Ultrasound-Guided Regional Anaesthesia: Visualising the Nerve and Needle. Adv Exp Med Biol. 2020;1235:19-34. doi: 10.1007/978-3-030-37639-0_2. PMID: 32488634.

[3] Karadsheh Z, Al-Haddad M. Endoscopic ultrasound guided fine needle tissue acquisition: where we stand in 2013? World J Gastroenterol. 2014 Mar 7;20(9):2176-85. doi: 10.3748/wjg.v20.i9.2176. PMID: 24605016; PMCID: PMC3942822.

[4] Baker, Christian, et al. Intraoperative Needle Tip Tracking with an Integrated Fibre-Optic Ultrasound Sensor. 2022, https://doi.org/10.3390/s22239035.

[5] Baker, C., et al. Real-Time Ultrasonic Tracking of an Intraoperative Needle Tip with Integrated Fibre-Optic Hydrophone. 2021 IEEE International Ultrasonics Symposium (IUS), 2021.

[6] Xia, Wenfeng, et al. "In-plane Ultrasonic Needle Tracking Using a Fiber-optic Hydrophone." Medical Physics (Lancaster), vol. 42, no. 10, 2015, pp. 5983–91, https://doi.org/10.1118/1.4931418.

[7] Langberg, J.J.; Franklin, J.O.; Landzberg, J.S.; Herre, J.M.; Kee, L.; Chin, M.C.; Bharati, S.; Lev, M.; Himelman, R.B.; Schiller, N.B.; et al. The echo-transponder electrode catheter: A new method for mapping the left ventricle. J. Am. Coll. Cardiol.

1988, 12, 218–223.

[8] Knott, P. D. (1990) The introduction of chorionic villus sampling as a screening test for Down's syndrome in older mothers. Thesis (MD) - King's college School of medicine and Dentistry, 1990.

[9] Boyd, P., DeVigan, C., Khoshnood, B., Loane, M., Garne, E., Dolk, H. and (2008), Survey of prenatal screening policies in Europe for structural malformations and chromosome anomalies, and their impact on detection and termination rates for neural tube defects and Down's syndrome. BJOG: An International Journal of Obstetrics & Gynaecology, 115: 689-696. https://doi.org/10.1111/j.1471-0528.2008.01700.x

[10] Ester Garne, Maria Loane, Diana Wellesley, Ingeborg Barisic, EUROCAT Working Group, Congenital hydronephrosis: Prenatal diagnosis and epidemiology in Europe, Journal of Pediatric Urology, Volume 5, Issue 1, 2009, Pages 47-52, ISSN 1477-5131, doi.org/10.1016/j.jpurol.2008.08.010.

[11] Niederstrasser, S. L. et al. (2017) Fetal loss following invasive prenatal testing: a comparison of transabdominal chorionic villus sampling, transcervical chorionic villus sampling and amniocentesis. Journal of perinatal medicine. [Online] 45 (2), 193–198.

[12] *Atlas of Ultrasound-Guided Procedures in Interventional Pain Management*. SPRINGER, 2019.

[13] G. A. Chapman, D. Johnson, and A. R. Bodenham, "Visualisation of needle position using ultrasonography," *Anaesthesia*, vol. 61, no. 2, pp. 148–158, 2006. doi:10.1111/j.1365-2044.2005.04475.x

[14] Jiang B, Struthers A, Sun Z, Feng Z, Zhao X, Zhao K, Dai W, Zhou X, Berens M E, Zhang L. Employing graphics processing unit technology, alternating direction implicit method and domain decomposition to speed up the numerical diffusion solver for the biomedical engineering research. *International Journal for Numerical Methods in Biomedical Engineering*, 2011, 27(11): 1829-1849. https://doi.org/10.1002/cnm.1444.

[15] Paul Y, Barthez D, Léveillé R, Peter V, Scrivani D. Side lobes and grating lobes artifacts in ultrasound imaging. *Veterinary Radiology & Ultrasound*, 1997, 38(5): 387-393. https://doi.org/10.1111/j.1740-8261.1997.tb02104.x.

[16] J. W. Charboneau, C. C. Reading, and T. J. Welch, "CT and sonographically guided needle biopsy: Current techniques and new innovations.,"*American Journal of Roentgenology*, vol. 154, no. 1, pp. 1–10, 1990. doi:10.2214/ajr.154.1.2104689

[17] C. C. Reading, J. W. Charboneau, J. P. Felmlee, and E. M. James, "US-guided percutaneous biopsy: Use of a screw biopsy stylet to aid needle detection.," *Radiology*, vol. 163, no. 1, pp. 280–281, 1987. doi:10.1148/radiology.163.1.3547495

[18] J. Gao, P. Liu, G.-D. Liu, and L. Zhang, "Robust needle localization and enhancement algorithm for ultrasound by deep learning and beam steering methods," *Journal of Computer Science and Technology*, vol. 36, no. 2, pp. 334–346, 2021. doi:10.1007/s11390-021-0861-7

[19] Jiang B N, Dai W Z, Khaliq A, Carey M, Zhou X B, Zhang L. Novel 3D GPU based numerical parallel diffusion algorithms in cylindrical coordinates for health care simulation. *Mathematics and Computers in Simulation*, 2015, 109: 1-19.

[20] Ren S, He K, Girshick R, Sun J. Faster R-CNN: Towards real-time object detection with region proposal networks. *IEEE Transactions on Pattern Analysis and Machine Intelligence*, 2017, 39(6): 1137-1149. https://doi.org/10.1109/TPAMI.2016.2577031.

[21] Xu Z, Huo Y, Park J, Landman B, Milkowski A, Grbic S, Zhou S. Less is more: Simultaneous view classification and landmark detection for abdominal ultrasound images. In *Proc. the 21st International Conference on Medical Image Computing and Computer-Assisted Intervention*, September 2018, pp.711-719. https://doi.org/10.1007/978-3-030-00934-2_79.

[22] Powers D. Evaluation: From precision, recall and F-factor to ROC, informedness, markedness & correlation. arXiv:2010.16061, 2008. https://arxiv.org/abs/2010.16061, Jan. 2021.

[23] Pourtaherian A, Ghazvinian Zanjani F, Zinger S, Mihajlovic N, Ng G C, Korsten H H M, De With P H N. Robust and semantic needle detection in 3D ultrasound using orthogonal-plane convolutional neural networks. *International Journal of Computer Assisted Radiology and Surgery*, 2018, 13(9): 1321-1333. https://doi.org/10.1007/s11548-018-1798-3.

[24] M. Najafi and R. Rohling, "Single camera closed-form real-time needle trajectory tracking for ultrasound," *SPIE Proceedings*, 2011. doi:10.1117/12.877798

[25] M. Baszyński, Z. Moroń, and N. Tewel, "Electromagnetic navigation in medicine – basic issues, advantages and shortcomings, prospects of improvement," *Journal of Physics: Conference Series*, vol. 238, p. 012056, 2010. doi:10.1088/1742 6596/238/1/012056

[26] Peters T, Cleary K. ,"Image-guided interventions," SpringerLink, https://link.springer.com/book/10.1007/978-0-387-73858-1 (accessed May 13,2023).

[27] S. Boutaleb *et al.*, "Performance and suitability assessment of a real-time 3D electromagnetic needle tracking system for interstitial brachytherapy," *Journal of Contemporary Brachytherapy*, vol. 4, pp. 280–289, 2015. doi:10.5114/jcb.2015.54062

[28] F. Stevens *et al.*, "Minimizing electromagnetic interference from surgical instruments on electromagnetic surgical navigation," *Clinical Orthopaedics & Related Research*, vol. 468, no. 8, pp. 2244–2250, 2010. doi:10.1007/s11999-010 1366-9

[29] M. A. Nixon, B. C. McCallum, W. R. Fright, and N. B. Price, "The effects of metals and interfering fields on electromagnetic trackers," *Presence: Teleoperators and Virtual Environments*, vol. 7, no. 2, pp. 204–218, 1998. doi:10.1162/105474698565587

[30] S. R. Kirsch, C. Schilling, and G. Brunner, "Assesment of metallic distortions of an electromagnetic tracking system," *SPIE Proceedings*, 2006. doi:10.1117/12.654768

[31] P. Beigi, S. E. Salcudean, G. C. Ng, and R. Rohling, "Enhancement of needle visualization and localization in ultrasound," *International Journal of Computer Assisted Radiology and Surgery*, vol. 16, no. 1, pp. 169–178, 2020. doi:10.1007/s11548-020-02227-7

[32] B. E. Treeby and B. T. Cox, "k-Wave: MATLAB toolbox for the simulation and reconstruction of photoacoustic wave-fields," J. Biomed. Opt., vol. 15, no. 2, p. 021314, 2010.

[33] C. Baker. "k-Wave simulation of the ultrasound needle tracking experimental setup", https://github.com/gift-surg/unt_sim (accessed Feb. 2 2023)

[34] Mwikirize C, Nosher J L, Hacihaliloglu I. Convolution neural networks for real-time needle detection and localization in 2D ultrasound[J]. International journal of computer assisted radiology and surgery, 2018, 13: 647-657.

[35] Mwikirize C, Kimbowa A B, Imanirakiza S, et al. Time-aware deep neural networks for needle tip localization in 2D ultrasound[J]. International Journal of Computer Assisted Radiology and Surgery, 2021, 16: 819-827.

[36] Groves L A, VanBerlo B, Peters T M, et al. Deep learning approach for automatic out-of-plane needle localisation for semi-automatic ultrasound probe calibration[J]. Healthcare technology letters, 2019, 6(6): 204-209.

[37] Gessert N, Priegnitz T, Saathoff T, et al. Needle tip force estimation using an oct fiber and a fused convgru-cnn architecture[C]//Medical Image Computing and Computer Assisted Intervention–MICCAI 2018: 21st International Conference, Granada, Spain, September 16-20, 2018, Proceedings, Part IV 11. Springer International Publishing, 2018: 222-229.

[38] Chen S, Lin Y, Li Z, et al. Automatic and accurate needle detection in 2D ultrasound during robot-assisted needle insertion process[J]. International Journal of Computer Assisted Radiology and Surgery, 2022: 1-9.

[39] Emerson M, Ferguson J M, Ertop T E, et al. A recurrent neural network approach to roll estimation for needle steering[C]//Experimental Robotics: The 17th International Symposium. Springer International Publishing, 2021: 334-342.

[40] Barkhaus P E, Roberts M M, Nandedkar S D. " Facial" and standard concentric needle electrodes are not interchangeable[J]. Electromyography and clinical neurophysiology, 2006, 46(5): 259-261.

[41] Sagi O, Rokach L. Ensemble learning: A survey[J]. Wiley Interdisciplinary Reviews: Data Mining and Knowledge Discovery, 2018, 8(4): e1249.

[42] Xia, W. *et al.* Looking beyond the imaging plane: 3D needle tracking with a linear array ultrasound probe. *Scientific Reports 2017 7:1* **7**, 1–9 (2017).

[43] Vrooijink, G. J., Abayazid, M. & Misra, S. Real-time three-dimensional flexible needle tracking using two-dimensional ultrasound. in *Proceedings - IEEE*

[44] Yeung, P. H., Aliasi, M., Haak, M., Xie, W. & Namburete, A. I. L. Adaptive 3D Localization of 2D Freehand Ultrasound Brain Images. *Lecture Notes in Computer Science (including subseries Lecture Notes in Artificial Intelligence and Lecture Notes in Bioinformatics)* **13434 LNCS**, 207–217 (2022).

[45] Prevost, R. *et al.* 3D freehand ultrasound without external tracking using deep learning. *Med Image Anal* **48**, 187–202 (2018).

[46] Chen, J.-F., Fowlkes, J. B., Carson, P. L. & Rubin, J. M. *Determination of Scan-Plane Motion Using Speckle Decorrelation: Theoretical Considerations and Initial Test*. *Int J Imaging Syst Technol* vol. 8 (1997).